Solid State Ionics 45 (1991) 201-213
North-Holland

Determination of niobium–oxygen bond distances and bond orders by Raman spectroscopy

Franklin D. Hardcastle [1] and Israel E. Wachs [2]
Zettlemoyer Center for Surface Studies, Departments of Chemistry and Chemical Engineering, Lehigh University, Bethlehem, PA 18015, USA

Received 21 May 1990; accepted for publication 22 October 1990

An empirical correlation is established for relating Raman stretching frequencies of niobium–oxygen (Nb–O) bonds to their respective bond distances in niobium oxide compounds. The correlation is an exponential least-squares fit between measured Raman frequencies and reported crystallographic bond lengths. Niobium–oxygen bond strengths (in valence units) are also related to Raman stretching frequencies by incorporating the present result with that of a previously derived bond strength/bond length relation. The Nb–O correlation established in the present study is expected to offer invaluable insight into the structures of niobate species in chemical systems which are not amenable to analysis by diffraction or other spectroscopic techniques. In the present study, applications of the correlation are illustrated by predicting Raman stretching frequencies for perfect NbO_4 and NbO_6 structures, determining the Nb–O bond lengths in bismuth niobate, $BiNbO_4$, as well as the bond length and bond strength of the terminal Nb=O bond for dehydrated surface niobate species in the Nb_2O_5/Al_2O_3 system.

1. Introduction

Raman spectroscopy yields much information when applied to the study of structures of transition metal oxides as bulk phases [1,2] and as two-dimensional surface phases [2,3]. This is because the Raman vibrational features depend on the symmetry and the bonding of the transition metal oxide complex and, consequently, can be used to discriminate between alternate molecular structures proposed for a given chemical species. For example, characteristic vibrational bands have been used to determine the tetrahedral coordination of surface rhenium oxide on an alumina support [4] and surface chromium oxide on alumina, titania, and silica supports [5].

Recently, empirical relations have been derived which relate vanadium–oxygen, molybdenum–oxygen, and bismuth–oxygen bond distances to observed Raman stretching frequencies in bulk transition-metal oxide reference compounds [6-8]. These empirical relations were justified by introducing the diatomic approximation where each metal–oxygen chemical bond is assumed to be a totally independent oscillator vibrationally separated from the rest of the molecule or the crystal lattice. According to the diatomic approximation, each distinct metal oxide polyhedron is reduced to an assembly of metal–oxygen diatomic functionalities. Each diatomic functionality, because it is vibrationally isolated, is characterized by its diatomic force constant and reduced mass. The force constant of a metal–oxygen bond is some function of its interatomic distance; that is, shorter covalent bonds are generally stronger than longer bonds. The dependence of force constant on interatomic distance may be approximated by a simple Morse potential energy function [9]. This treatment results in an exponential relation between Raman stretching frequency and bond distance, where the pre-exponential and exponential factors are empirically derived. A stretching frequency/bond distance correlation may be used to estimate bond distances in metal oxides of unknown structures from their measured Raman frequencies.

---

[1] Present address: Div. 1845, Sandia National Laboratories, Albuquerque, New Mexico 87185, USA.
[2] Author to whom all correspondence should be addressed.

In the present study, an empirical expression is determined which relates the niobium–oxygen (Nb–O) crystallographic bond distances to Raman stretching frequencies. Plots are presented showing the behavior of the Nb–O bond distance and bond order as a function of Nb–O stretching frequency. These relationships are expected to offer insight into the structures of niobate species in chemical systems for which diffraction techniques provide incomplete structural information.

2. Experimental

The Raman spectra of the following niobate reference compounds were collected in our laboratory: $LiNbO_3$, $NaNbO_3$, $KNbO_3$, $AlNbO_4$, $H_2(NbO(OH)(C_2O_4)_2H_2O)4H_2O$, and Nb_2O_5 (high-temperature form). The Raman band positions of $SbNbO_4$ [10], $NbOPO_4$ [11], $YNbO_4$ [12], and $CaNb_2O_6$ [13] were taken from the literature.

The Raman spectra were obtained with a Spectra-Physics Ar^+ laser (Model 171) by utilizing about 10–40 mW of the 514.5-nm line for excitation. The laser intensity was monitored at the sample. The scattered radiation from the sample was directed into a Spex Triplemate Spectrometer (Model 1877), where the Raman spectra were detected with an intensified photodiode array (1024 pixels) via an optical multichannel analyzer (OMA III: Princeton Applied Research, Model 1463). The photodiode array was thermo-electrically cooled to $-35°C$. The Raman spectra were collected and recorded using an OMA III (PAR) dedicated computer and software. The spectral resolution and reproducibility was experimentally determined to be better than 2 cm^{-1}. About 100–200 mg of each niobium oxide reference compound was pressed into a thin wafer of about 1 mm thickness with a KBr backing for support. Each sample was then mounted onto a spinning sample holder and rotated at ~ 2000 rpm to avoid local heating effects. A 90° collection geometry was used to collect the scattered light. Further details concerning the optical arrangement used in the Raman experiments can be found elsewhere [3].

3. Theory

3.1. The diatomic approximation

The Raman spectrum of a metal oxide molecule contains detailed structural information because the Raman vibrational modes are determined by the symmetry and bonding of the molecular species [1]. The symmetry and bonding of the molecule may be significantly altered, however, if the environment of the molecule is changed. For example, when the molecule is confined within a crystalline lattice its vibrational spectrum differs from that of the same molecule in free space or in solution because the site symmetry of the metal cation is usually lower in the crystalline state. Furthermore, the confined molecule is an integral part of the entire array of atoms constituting the lattice. In addition to the internal modes of the molecular unit, external modes are expected to occur reflecting the translational and librational nature of the crystalline lattice. A rigorous vibrational mode analysis must account for all atoms constituting the array. Often, however, such an approach is computationally unfeasible and unnecessary. Instead, approximations are made in order to correlate the vibrational spectrum of the molecular unit in the crystal with that of the same molecular unit in the gas or solution phase.

The diatomic approximation allows a straightforward interpretation of the Raman spectrum of a crystalline metal oxide compound. It assumes that each distinct metal–oxygen bond is entirely separated from the crystalline lattice. Such a separation means that there are no vibrational interactions between neighboring metal–oxygen bonds in the lattice. To a first approximation, the Raman spectrum of the crystalline compound is a superposition of stretching frequencies directly reflecting the distinct metal–oxygen bonds constituting the lattice. For any given metal oxide, the diatomic approximation assumes that each stretching frequency observed in the Raman spectrum is characterized only by the bond length of the metal–oxygen bond it represents.

In the present study, the diatomic approximation is used to justify the empirical relation between niobium–oxygen (Nb–O) bond distances and Raman stretching frequencies. The functional dependence of the bond length on the stretching frequencies is approximated from the Morse potential energy function [9] to be exponential. This approach has recently been used to derive such bond length/stretching frequency relations for vanadium-oxygen [6], molybdenum-oxygen [7], bismuth-oxygen [8], and tungsten-oxygen [14] bonds. The Nb-O bond strength (in valence units) is also related to Raman stretching frequencies by using an empirical relationship from Brown and Wu [15] which relates Nb-O bond distances to bond orders.

3.2. Relating stretching frequencies to bond distances

Many empirical and semi-empirical formulae have been developed for simple diatomic molecules [16-18]. These expressions describe interdependencies of physical parameters such as bond distances, force constants, and bond valencies. Recent efforts at relating force constants to bond distances for diatomic molecules have also been extended to polyatomic molecules. Perhaps the most common expression relating bond lengths to force constants in diatomic and polyatomic molecules is Badger's rule [19]. Badger's rule takes the general form

$$k^{-1/3}=(a_{ij}-d_{ij})^{-1}(R-d_{ij}), \qquad (1)$$

where k (mdynes/Å) is the force constant, R (Å) is the equilibrium bond length, and d_{ij} and a_{ij} are constants which are fixed for designated bonds between atoms from rows i and j of the periodic table. Badger's rule has recently been used to correlate uranium-oxygen bond lengths with symmetric and antisymmetric stretching frequencies of dioxo-functionalities (UO_2) in uranium oxide compounds [20].

In the course of present work, it was found that Badger's rule does not adequately correlate Nb-O bond distances to force constants in niobate reference compounds. In fact, significant curvature from Badger's linear relationship is observed for the several transition metal oxide systems investigated. This deviation from Badger's rule demands application of a more appropriate mathematical form. Herschbach [19] found such deviations to be generally present in fitting cubic and quartic vibrational force constants to internuclear distances for diatomic molecules. Consequently, Herschbach applied an exponential relationship to account for the curved nature of the data. A similar approach is used in the present study for fitting Nb-O stretching frequencies (force constants) to their respective bond distances. The exponential function used in the present study assumes the general form

$$\nu=A\exp(BR) . \qquad (2)$$

In this function ν is the Nb-O stretching frequency, R is the Nb-O bond distance, and A and B are fitting parameters. Eq. (2) may also be arrived at by estimating the force constant from the Morse potential energy function [9]. In the present study, the fitting parameters are determined from an exponential least-squares fit of the crystallographic and Raman data from several niobium oxide reference compounds.

Pauling's valence sum rule is a useful concept for discussing the feasibility of a proposed niobate structure [21]. The valence sum rule states that the sum of the individual Nb-O bond valences, or bond orders, equals the formal oxidation state of the niobium cation, or 5.0 valence units (v.u.) in the case of a Nb^{5+}. A chemical bonds' valency is a measure of its strength and shows the distribution of available valence electrons throughout its covalent structure. Hence, the Nb-O bond order and calculated valence state of the niobium cation serve as a bookkeeping device for valence electrons at a niobium cation site as well as a check on the feasibility of a proposed niobate structure. Brown and Wu [15] developed a generally applicable relationship between the metal-oxygen bond valence s and the bond distance R. The empirical expression relating Nb-O bond distance to bond valency is

$$s(\mathrm{Nb{-}O})\approx(R/1.907)^{-5.0}, \qquad (3)$$

where 1.907 is the estimated bond length for an Nb-O bond of unit valency. From the calculated valencies of the Nb-O bonds of any Nb site, the valence sum rule can be used to estimate the valence state of the Nb cation.

4. Results

The Nb-O bond distances were obtained from several niobium oxide reference compounds and correlated with their corresponding Raman stretching frequencies. The reference compounds are listed in table 1 along with the crystallographically determined Nb–O bond distances, corresponding literature references, assigned Raman stretching frequencies, bond strengths calculated from eq. (3), valence state of the niobium cation(s) from the valence sum rule, and the coordination number of each niobium cation to oxygen.

The procedure for assigning the Raman stretching frequencies to Nb–O bonds in the niobate reference compounds is as follows. First, the short Nb–O bonds of the reference compounds were correlated with their

Table 1

Bond distances and observed stretching frequencies for Nb–O bonds in niobium oxide reference compounds. s = Calculated valency of Nb–O bond (eq. (3)); Nb v.s.: Calculated valence state of Nb cation; relative error is 3%; C.N.: Coordination number of Nb cation; ν(cm^{-1}): Assigned Nb–O stretching frequency.

Compound		R (Å)	ν (cm^{-1})	s	Nb v.s.	CN	Ref.
$LiNbO_3$	(3x)	1.889	680	1.05			[22]
	(3x)	2.112	432	0.60	5.0	6	
$SbNbO_4$		1.809	740	1.30			[10,27]
		1.879	718	1.08			
		2.006	542	0.78			
		2.076	448	0.65			
	(2x)	2.125	448	0.58	5.0	6	
$NbOPO_4$	(1x)	1.783	800	1.40			[11,35]
	(4x)	1.969	612	0.85			
	(1x)	2.321	290	0.37	5.2	6	
$NaNbO_3$		1.857	800	1.14			[36]
		1.950	600	0.89			
		1.967	600	0.86			
		1.980	580	0.83			
		2.049	559	0.70			
		2.110	432	0.60	5.0	6	
$KNbO_3$	(2x)	1.870	832	1.10			[37]
	(2x)	1.991	598	0.81			
	(2x)	2.170	415	0.52	4.9	6	
$YNbO_4$	(2x)	1.824	832	1.25			[12,38]
	(2x)	1.917	650	0.97			
	(2x)	2.415	245	0.31	5.1	6	
$CaNb_2O_6$		1.77	904	1.45			[13]
		1.92	664	0.97			
		1.95	638	0.89			
		2.06	495	0.68			
		2.08	484	0.65			
		2.34	286	0.36	5.0	6	
$AlNbO_4$	(a)	1.749	932	1.54			[39]
	(b)	1.758	932	1.50			
	(a)	1.825	793	1.25			
	(b)	1.856	722	1.15			
	(aa)	1.941	590	0.92			
	(bb)	1.950	590	0.89			
	(a)	2.012	530	0.76			
	(a)	2.155	418	0.54			
	(b)	2.195	418	0.49	(a) 5.9	6	
	(b)	2.290	339	0.40	(b) 5.3	6	

Table 1 (continued)

Compound		R (Å)	ν (cm^{-1})	s	Nb	v.s.	CN	Ref.
$H_2(NbO(OH)(C_2O_4)_2H_2O)4H_2O$		1.66	958	2.00				[26]
		2.07	477	0.66				
		2.10	477	0.62				
		2.11	477	0.60				
		2.12	477	0.59				
		2.29	326	0.40		4.9	6	
H-Nb_2O_5	(*aa*)[a]	1.65	993	2.06				[23]
	(*aa*)	1.68	993	1.88				
	(*n*)	1.73	993	1.63				
	(*i*)	1.77	898	1.45				
	(*m*)	1.79	843	1.37				
	(*jk*)	1.80	843	1.33				
	(*i*)	1.81	820	1.30				
	(*hm*)	1.82	820	1.26				
	(*dgl*)	1.84	760	1.20				
	(*efjl*)	1.85	760	1.16				
	(*ho*)	1.89	674	1.05				
	(*bboo*)	1.91	674	0.99				
	(*ccdef*)	1.92	663	0.97				
	(*h*)	1.95	627	0.89				
	(*c*)	1.96	613	0.87				
	(*bb*)	1.97	613	0.85				
	(*cdgmm*)	1.98	549	0.83				
	(*bb*)	1.99	549	0.81				
	(*gjknnno*)	2.00	549	0.79				
	(*eff*)	2.01	549	0.77	(*a*)	7.9	4	
	(*gghhln*)	2.02	549	0.75	(*b*)	5.3	6	
	(*eeo*)	2.03	549	0.73	(*c*)	4.7	6	
	(*eiikkk*)	2.04	549	0.71	(*d*)	5.0	6	
	(*dddjjm*)	2.06	470	0.68	(*e*)	5.1	6	
	(*k*)	2.07	470	0.66	(*f*)	4.7	6	
	(*ll*)	2.09	470	0.63	(*g*)	4.8	6	
	(*m*)	2.11	470	0.60	(*h*)	5.1	6	
	(*fijo*)	2.14	394	0.56	(*i*)	5.2	6	
	(*cg*)	2.16	394	0.54	(*j*)	5.2	6	
	(*c*)	2.17	394	0.52	(*k*)	4.9	6	
	(*f*)	2.19	394	0.50	(*l*)	4.8	6	
	(*il*)	2.24	345	0.45	(*m*)	5.6	6	
	(*n*)	2.26	345	0.43	(*m*)	5.2	6	
	(*h*)	2.31	307	0.38	(*o*)	5.1	6	

[a] Letters in parenthesis designate crystallographically distinct Nb sites.

stretching frequencies. The short Nb–O bonds vibrate at the highest frequencies, > 800 cm^{-1}, and are therefore the most obvious to assign. A preliminary least-squares exponential fit of the data for the short Nb–O bonds was performed using eq. (2). Next, the Nb–O bonds of intermediate length were correlated to their stretching frequencies, found in the ~800–400 cm^{-1} region, by extrapolating from the short Nb–O bonds using the preliminary exponential fit. This procedure was repeated for the longer Nb–O bonds where the stretching frequencies are in the low-frequency region, <400 cm^{-1}. The assignment of Nb–O bonds to Raman stretching frequencies in this region is somewhat tenuous because of the large number of bands usually present in this wavenumber region; for example, from internal bending and lattice vibrations. Nevertheless, the long Nb–O bonds were correlated to stretching frequencies by extrapolation, and a refined Nb–O correlation was determined based on all available data points.

A complication which arises in the assignment of Nb–O bond distances to Raman stretching frequencies is that not all Raman bands present in the Raman spectrum of a crystalline niobium oxide compound are assigned to Nb–O diatomic functionalities because some Raman bands are symmetry related. This complication is especially evident in the assignment of the longer Nb–O bonds. The symmetry-related bands result from internal or external modes involving groups of three or more atoms present in the crystal, and these modes are not accounted for in the diatomic approximation. For example, internal modes resulting from vibrational interactions between neighboring chemical bonds in chemical functionalities such as NbO_2 and NbO_3, as well as external modes due to the space-group symmetry of the crystal, do not directly relate to bond distances by the Nb–O correlation.

A range of niobate structures are represented by several niobium oxide reference compounds, and these are listed in table 1. All of these compounds consist of NbO_6 octahedra because niobium oxide reference compounds containing NbO_4 tetrahedra are rare. A general conclusion made from comparing the Raman spectra of complex transition metal oxides is that the lower the stretching frequency for the shortest metal–oxygen bonds, the more regular is the structure. Consequently, the niobate reference compounds in table 1 are listed in order of increasing highest stretching frequency and reflects the relative regularity of the NbO_6 structures in these niobium oxide reference compounds. Accordingly, $LiNbO_3$ [22] has the most ordered octahedron while the high-temperature modification of Nb_2O_5 [23] contains

Table 2
Nb–O stretches, symmetry-related, and extraneous Raman bands of niobium oxide reference compounds.

Compound	Nb–O stretches	Symmetry-related	Extraneous
$LiNbO_3$	680, 432	876, 628, 582, 370, 322, 308, 276, 256, 238, 180, 152	
$SbNbO_4$	740, 718, 542, 448	913(vw), 397, 377, 350, 292, 269, 239, 232, 192, 168, 128, 87	620 (SbO_5)
$NbOPO_4$	800, 612, 290, 375	385	1016, 980, 445, (PO_4)
$NaNbO_3$	800, 600, 580, 559, 432	667, 385, 325, 275, 257, 219, 184, 154, 144, 123	
$KNbO_3$	832, 598, 415	531, 294, 279, 192	
$YNbO_4$	832, 650, 245	715, 695, 675, 560, 480, 455, 435, 385, 350, 340, 225, 170	
$CaNb_2O_6$	904, 664, 638, 495, 484, 286	540, 379, 241, 225, 195, 139, 64 (A_g species)	
$AlNbO_4$	932, 793, 722, 590, 530, 418, 339	287, 244, 215, 182, 140	
Niobium oxalate [a]	958, 477, 326	386, 362, 345, 303, 284, 242, 195, 155, 147	928, 849, 798, 572, 552 (oxalate)
H-Nb_2O_5	993, 898, 843, 820, 760, 674, 663, 627, 613, 549, 470, 394, 345, 307	287, 262, 246, 238, 207, 182, 159, 136	

[a] $H_2(NbO(OH)(C_2O_4)_2H_2O)4H_2O$.

the most irregular structure. Incidentely, this highly distorted structure is an NbO_4 tetrahedron which occurs in one out of every twenty five Nb cations in the H-Nb_2O_5 structure.

Symmetry-related Raman stretching modes, as well as extraneous Raman bands resulting from other molecular moities contained within the crystalline lattices, are tabulated in table 2. In almost all cases, the high-frequency bands are assigned to Nb–O stretches unless a high degree of point-group symmetry is present or other molecular moities are present. $LiNbO_3$ possesses a high degree of point-group symmetry, with only two sets of Nb–O bond lengths, and the highest-frequency mode at 876 cm^{-1} does not correlate with the shortest Nb–O bond length. In contrast, the highest-frequency bands to $NaNbO_3$ and $KNbO_3$ at 800 and 832 cm^{-1}, respectively, are assigned to their shortest Nb–O bonds. A few reference compounds exhibit Raman bands characteristic of non-niobate functionalities. For example, the high-frequency Raman bands of $NbOPO_4$ at 1016, 980, 445, and 375 cm^{-1} have been assigned to PO_4 tetrahedra [11] while those of $H_2(NbO(OH)(C_2O_4)_2H_2O)4H_2O$ at 928, 849 and 798 cm^{-1} are characteristic of the oxalic acid groups.

The data from table 1 consist of 78 data points correlating Nb–O stretching frequencies to crystallographic Nb–O bond distances from the literature. The Nb–O correlation, resulting from a least-squares exponential fit of the data, is found to be

$$\nu(\mathrm{cm}^{-1}) = 25\,922 \exp(-1.9168\,R). \qquad (4)$$

The precision in estimating a Nb–O bond distance from the Nb–O correlation, given an absolute stretching frequency, is ±0.024 Å. The standard deviation associated with the calculation of a stretching frequency from an Nb–O bond distance is ±30 cm^{-1}. The data points and the above Nb–O correlation, eq.(4), are plotted in fig. 1. Bond order/stretching frequency correlations are also useful in the determination of niobate structures because the Nb–O bond order is representative of the strength of the chemical bond. A relationship between Nb–O bond strength (in valence units) and Nb–O Raman stretching frequency is easily derived from eqs.(3) and (4):

$$s(\mathrm{Nb{-}O}) = 653\{\ln[25\,922/\nu(\mathrm{cm}^{-1})]\}^{-5.0}. \qquad (5)$$

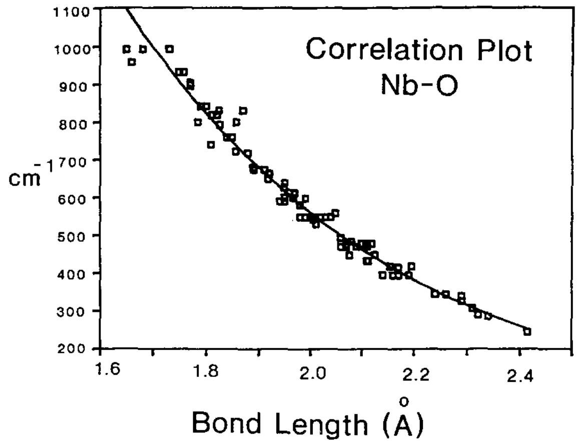

Fig. 1. Nb–O correlation plot relating bond distance (Å) to stretching frequency (cm^{-1}). The 78 data points are fit to the exponential function $\nu(\mathrm{cm}^{-1}) = 25\,922 \exp(-1.9168\,R)$, where R is the bond distance in ångströms.

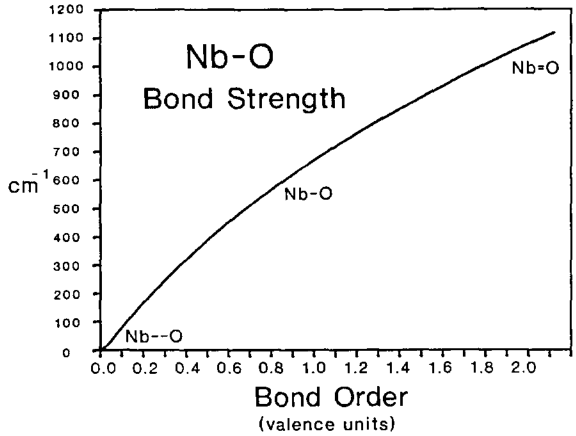

Fig. 2. Correlation plot relating Nb–O bond order (valence units) to Nb–O stretching frequency (cm^{-1}).

A plot showing the relationship between Nb–O bond strength and stretching frequency is presented in fig. 2.

5. Discussion

The Nb–O correlation is derived from a least-squares exponential fit of the crystallographically determined bond distances and observed Raman stretching frequencies. Such a direct relationship between these two experimental observables is justified under the assumptions of the diatomic approximation and an anharmonic dependence between force constant and interatomic distance. The basic assumption behind fitting the data in table 1 to eq. (2), which is estimated from the Morse energy function, is that each distinct Nb–O bond is vibrationally isolated from its environment. Each isolated Nb–O bond exhibits a stretching frequency which is characteristic of its bond length within the limits of experimental uncertainty. To a first approximation, the Raman spectrum of the niobate compound is a superposition of Nb–O stretching frequencies. Raman bands appearing in the spectrum which cannot be correlated to Nb–O bond lengths are due to symmetry-related modes. Raman bands arising from symmetry-related modes almost always occur at low frequency, $< 300\ \mathrm{cm}^{-1}$, but seldom occur at high frequencies. Exceptions occur for molecules confined to a crystalline lattice and possessing a high degree of point-group symmetry.

The reasoning behind the diatomic approximation is very different from that of the site symmetry approximation [6]. The site symmetry approximation assumes that a high degree of symmetry is present at the Nb site, usually more than is actually present. The diatomic approximation, because it assumes that all Nb–O oscillators are vibrationally independent, disregards the site symmetry at the Nb cation site. Thus, both of these approaches begin with an assumption concerning the site symmetry of the Nb cation: the diatomic approximation assumes no site symmetry while the site symmetry approximation assumes high site symmetry. Certainly, if possible, both approaches should be used in order to attain a thorough understanding of the vibrational spectrum in terms of the complete structure of the niobium oxide compound. The diatomic approximation may be used to unambiguously assign all Nb–O stretching vibrations, and this information may be used as the starting point for assigning the remaining bands by the site symmetry approach. Finally, the combined information thus obtained may be utilized in an intricate vibrational mode analysis.

Several applications of the Nb–O correlation will be demonstrated below. The versatility of the correlation allows the prediction of the stretching frequencies of highly symmetric niobium oxide species, such as the perfect NbO_4 tetrahedron and the perfect NbO_6 octahedron, as well as the determination of Nb–O bond lengths in bulk materials. Perhaps the most beneficial application of the Nb–O correlation is in the determination of the coordination and Nb–O bond lengths of niobate species in materials which are diffraction amorphous; such a system is depicted by the dehydrated surface niobate species.

5.1. Applications

5.1.1. Determining stretching frequencies for ideal structures: NbO_4 and NbO_6

An interesting application of the Nb–O correlation is the prediction of Raman stretching frequencies for proposed niobate structures. The stretching frequencies for the perfect NbO_4 tetrahedron and NbO_6 octahedron can be estimated from the Nb–O correlation. These ideal structures have a high degree of point-group symmetry (T_d and O_h, respectively). Consequently, vibrational interactions between bonds are expected to be significant; for example, stretch–stretch interaction constants are roughly one-tenth of the stretching force constant [24]. In spite of strong vibrational interactions, the diatomic approximation may be used to provide an excellent estimate of the frequency of the totally symmetric Nb–O stretching mode for each of these structures. This is because the magnitude of the vibrational interaction constants between neighboring Nb–O bonds is smaller than the experimental error associated with the crystallographic measurements of Nb–O bond distances and Raman stretching frequencies. The stretching frequencies of the regular NbO_4 and NbO_6 structures are estimated by first equally dividing the five valence units of bond order between the four bonds of the tetrahedron and the six bonds of the octahedron. This results in Nb–O bond lengths of 1.823 and 1.977 Å for the NbO_4 and NbO_6 structures, respectively, by eq. (3). If these bond distances are considered absolute (without error), then the Nb–O correlation, eq. (4), yields stretching frequencies of 787 cm^{-1} for the perfect NbO_4 tetrahedron and 586 cm^{-1} for the perfect NbO_6 octahedron. The predicted stretching frequencies have a standard deviation of $\pm 30\ \mathrm{cm}^{-1}$ reflected in the overall precision of eq. (4). Thus, we expect 787 and 586 cm^{-1} to approximate the stretching frequencies for the perfect NbO_4 and NbO_6 structures, respectively.

A comparison of the stretching frequencies of those predicted for the perfect NbO_4 and NbO_6 structures with those of existing niobate compounds suggests that these perfect structures may not exist. The only NbO_4 tetrahedron listed in table 1 is present in H-Nb_2O_5, however this structure is highly distorted with two reported bond lengths of 1.65 Å and two of 1.68 Å [23]. Incidentely, the calculated valence state of the Nb^{5+} cation for the NbO_4 tetrahedron is 7.9 v.u., well beyond the limit of the 3% relative error allowed for the calculation of the Nb^{5+} valence state (5.0 ± 0.16v.u.). This very high calculated valence state for the NbO_4 tetrahedron is H-Nb_2O_5 indicates that the reported bond lengths for this structure are not correct. In general, niobium does not readily form NbO_4 structures which explains why such compounds are rare. According to a simple "radius ratio" [25] argument, the closest-packing of O^{2-} ions around a Nb^{5+} ion leads to a ratio for preferred tetrahedral coordination of 0.225, while that for octahedral coordination is 0.414. The ratio of the Nb^{5+} ionic radius to the O^{2-} ionic radius is 0.70/1.40, or 0.5, suggesting that the Nb^{5+} cation is too large to accommodate tetrahedral coordination and the NbO_6 arrangement is preferred.

The most regular niobate octahedron listed in table 1 is that of the $LiNbO_3$ structure. The Raman stretching frequency of the shortest Nb-O bond occurs at only 680 cm^{-1}. This value is 94 cm^{-1} higher than the value of 586 cm^{-1} for the ideal NbO_6 octahedron. The most distorted octahedron is that of niobium oxalate, $H_2(NbO(OH)(C_2O_4)_2H_2O)4H_2O$ [26], which has a very short Nb=O bond of length 1.66 Å and bond strength 2.0 v.u., and it exhibits a stretching band as high as 958 cm^{-1}.

5.1.2. *Determining the structure of bulk metal oxides: $BiNbO_4$*

The Nb-O correlation, eq.(4), may also be used to determine the most probable Nb-O bond lengths for a niobate structural unit. In this section, the Nb-O bond lengths for the NbO_6 octahedron in bismuth niobate, $BiNbO_4$, are determined from its Raman spectrum. The structure of bismuth niobate is directly compared to that of antimony niobate, $SbNbO_4$, because the unit-cell dimensions for both materials are quite comparable [27]. Furthermore, their Raman spectra are almost identical [10], and this indicates that the structures of the NbO_6 octahedra in both $SbNbO_4$ and $BiNbO_4$ are similar. The Nb-O bond lengths of the NbO_6 octahedron in $BiNbO_4$ may be determined by directly comparing its Raman spectrum with that of the isostructural $SbNbO_4$, for which both the Nb-O bond lengths and the Raman stretching assignments are known (tables 1 and 2). Finally, the corresponding Raman stretching frequencies for $BiNbO_4$ are converted to Nb-O bond lengths by eq. (4).

The observed Raman bands for $BiNbO_4$ are at 882, 726, 616, 530, 418 and 365 cm^{-1} [8]. The Raman bands of $SbNbO_4$, which are related to the Nb-O bond lengths of the NbO_6 octahedra in $SbNbO_4$, are 740, 718, 542 and 448 cm^{-1} [10]. By comparison, the corresponding band positions of $BiNbO_4$, which are expected to yield bond distance information, are 726, 530 and 418 cm^{-1}. These Raman stretching frequencies are converted to Nb-O bond strengths of of 1.118, 0.733 and 0.545 v.u. by eqs.(3) and (4). Two Nb-O bonds of each bond order give a calculated niobium valence of 4.8 v.u. which is at the lower extreme of the ±0.2 v.u. tolerance. This value is improved by including the high-frequency band at 882 cm^{-1} as a Nb-O stretching mode. This band at 882 cm^{-1} is converted to a bond order of 1.476 v.u. As a result, a valence sum of 5.1 ± 0.2 v.u. is attained by Nb-O bonds of strength 1.476, 1.118, 0.733, 0.545 and 0.545 v.u. The Raman bands corresponding to these bond strengths are at 882, 726, 530 and 418 cm^{-1}. Finally, the Raman bands for $BiNbO_4$ are converted to Nb-O bond lengths of 1.764, 1.865, 2.029, 2.029, 2.153 and 2.153 Å by eq.(4); all bond lengths have a precision of ±0.024 Å. The Nb-O bond lengths of $BiNbO_4$ and $SbNbO_4$ are compared in table 3.

Of special note is the intense band at ~622 cm^{-1} observed in the Raman spectra of both $BiNbO_4$ and $SbNbO_4$. At first guess, this band may be assigned as a symmetry-related mode because it does not directly reflect Nb-O bond lengths. This band, however, may reflect the shortest bonds of the BiO_5 and SbO_5 polyhedra present in these structures. In the case of $BiNbO_4$, for example, the structure of the BiO_5 polyhedron may be similar to that observed in the

Table 3
Nb-O bond lengths of NbO_6 octahedra in $BiNbO_4$ and $SbNbO_4$.

	$BiNbO_4$ [a] (±0.02 Å)	$SbNbO_4$ [b] (±0.009 Å)
Nb-O	1.76	1.809
-O	1.86	1.879
-O	2.03	2.006
-O	2.03	2.076
-O	2.15	2.125
-O	2.15	2.125

[a] Determined from Raman positions.
[b] From ref. [27].

BiO_5 building blocks of the sillenite-type structures [28] where a high-frequency band is observed at ~625 cm^{-1} and corresponds to a Bi-O bond length and strength of about 2.1 Å and 0.85 v.u. Thus, in the case of $BiNbO_4$ and $SbNbO_4$, the strong Raman band at ~622 cm^{-1} may be due to the BiO_5 and SbO_5 polyhedra in these structures and not to a symmetry-related mode.

5.1.3. Determining the structure of surface metal oxides: Nb_2O_5/Al_2O_3

The determination of bond distances from Raman stretching frequencies is of most benefit when diffraction techniques are unable to detect oxygen positions because of the absence of long-range order. Such is the case for supported metal oxides which are present as two-dimensional surface oxides on high surface-area metal oxide substrates. One example of a surface metal oxide is the dehydrated surface niobate species supported on alumina, Nb_2O_5/Al_2O_3. This system has not been previously reported in the literature, but has been investigated by our laboratory [29].

The Raman spectra for a hydrated (ambient) and dehydrated 12 wt% Nb_2O_5/Al_2O_3 system (63% of a monolayer) exhibits a very strong band at ~900 cm^{-1} and a weaker band at 650 cm^{-1} [29]. As the Nb_2O_5 loading is increased to monolayer coverage, the relative intensity of the band at 650 cm^{-1} increases with respect to that of the band at ~900 cm^{-1}. The 650 cm^{-1} band is due to the Nb-O stretching of slightly distorted NbO_6 units similar to those found in the layers of amorphous $Nb_2O_5 \cdot nH_2O$ [30]. The value of 650 cm^{-1} is converted to a Nb-O bond distance of 1.92±0.02 Å and a bond strength of about 0.96 v.u. In the previous section, the perfect NbO_6 octahedron was estimated to have an Nb-O bond length of 1.98±0.02 Å and a Raman stretching frequency of 586±30 cm^{-1}. The precision in these estimates allows extreme values of 1.96 Å and 616 cm^{-1} for the perfect NbO_6 octahedron, still out of range for the extreme values of 1.94 Å and 650 cm^{-1} observed for the Nb_2O_5/Al_2O_3 system. Thus, the 650 cm^{-1} Raman band observed for the surface niobate species is due the Nb-O stretch of a *slightly distorted* NbO_6 octahedron, with one or more short Nb-O bonds of 1.92±0.02 Å.

The intense band at ~900 cm^{-1} in the Raman spectrum of the hydrated surface niobate species [29] is due to a highly distorted NbO_6 octahedron of an aqueous $H_xNb_6O_{19}{}^{(8-x)-}$ surface species. This conclusion is drawn by comparing the Raman spectra of known aqueous niobate reference compounds [31] with the spectrum of the hydrated surface niobate species. The surface $H_xNb_6O_{19}{}^{(8-x)-}$ polyoxoanion is expected to be nearly non-interacting with the alumina surface because of the high concentration of water on the surface. In this regard the alumina surface may be simply considered as a microcontainer for the aqueous niobate solution. This fingerprint approach at identifying hydrated surface species has recently proven valuable in identifying hydrated surface rhenium oxide [4] and chromium oxide [5] species.

In situ dehydration of the Nb_2O_5/Al_2O_3 system causes degradation of the surface $H_xNb_6O_{19}{}^{(8-x)-}$ polyoxoanion but not the slightly distorted NbO_6 octahedra. This observation confirms that the structure of the surface $H_xNb_6O_{19}{}^{(8-x)-}$ polyoxoanion depends on moisture, whereas the slightly distorted NbO_6 octahedron does not depend on moisture and is likely present as a bulk species in the alumina support. As indicated above, the Raman band at 650 cm^{-1} matches that of the slightly distorted NbO_6 octahedra present in amorphous $Nb_2O_5 \cdot nH_2O$ [30]. Upon dehydration, the band at ~900 cm^{-1}, for the surface $H_xNb_6O_{19}{}^{(8-x)-}$ polyoxoanion, splits into two broad bands at 935 and 883 cm^{-1} and one sharp band at 985 cm^{-1} [29]. Splitting of this Raman band is also observed for aqueous niobate systems as the *pH* of the solution is decreased, but is accompanied by a sharp band in the 728-786 cm^{-1} region [31]. This expected Raman band, however, is not observed in the Raman spectrum of the dehydrated surface niobate species on alumina [29]. Failure to observe this diagnostic band in the 728–786 cm^{-1} region indicates that the transformation of the surface $H_xNb_6O_{19}^{(8-x)-}$ polyoxoanion is not regulated by a simple equilibrium process. The inconsistent band shapes in the Raman spectrum, one sharp and two broad bands, further indicate that the surface $H_xNb_6O_{19}^{(8-x)-}$ polyoxoanion has degraded to two or more surface species upon dehydration.

The two sets of Raman bands, which appear upon degradation of the surface $H_xNb_6O_{19}^{(8-x)-}$ polyoxoanion, consist of two broad bands at 883 and 935 cm^{-1} and one very sharp band at 985 cm^{-1}. The broad bands at 883 and 935 cm^{-1} are consistent with the Raman bands observed for $K_9H_3Nb_{12}O_{36}\cdot 28H_2O$ at 870, 895 and 920 cm^{-1} [32]. Thus, it is conceivable that a fraction of the surface $H_xNb_6O_{19}^{(8-x)-}$ polyoxoanions have undergone condensation to form $Nb_{12}O_{36}$-like surface species. The remaining surface niobate species are responsible for the very sharp Raman band at 985 cm^{-1}. This frequency is very high and indicates a highly distorted surface species. The 985 cm^{-1} band cannot be a symmetry-related band because the niobate species is highly distorted and is present as a two-dimensional surface species. High-frequency, symmetry-related Raman bands are typically observed for symmetric species which are confined to an ordered crystalline lattice; that is, where both point-group and space group symmetry is present.

It is readily shown, using eqs.(3)–(5), that the highly distorted surface niobate species, exhibiting an Nb–O stretch at 985 cm^{-1}, is a mono-oxo species; that is, the highly distorted niobate species terminates with one Nb=O bond. The bond length and strength of this terminal Nb=O bond is found to be 1.706±0.024 Å and 1.75 v.u. from eqs.(3)–(5). If the niobate species were dioxo-, having two terminal Nb=O bonds, then this would account for 3.5. v.u. of the available 5.0 v.u. for valence bonding to oxygen. If an NbO_4 tetrahedral model were assumed, then each bridging Nb–O bond strength for the mono-oxo species would be 1.08 v.u., and for the dioxo species would be only 0.75 v.u. Metal–oxygen–metal linkages of tetrahedrally coordinated species, however, have bond strengths of about unit valency (see table 1) [6] and this is consistent with the mono-oxo NbO_4 tetrahedron but not the dioxo tetrahedron. If an NbO_6 octahedral model were assumed, then each bridging Nb–O bond would average 0.65 v.u. for the mono-oxo species and 0.38 v.u. for the dioxo species. Clearly, there are not enough valence electrons to sustain a dioxo NbO_6 octahedron. For a typical mono-oxo NbO_6 octahedron, however, there is one short apical bond, an opposing very long Nb--O bond, and four intermediate Nb–O bridging bonds. The short apical Nb=O bonds, of length 1.706±0.024 Å and strength 1.75 v.u., has an opposing Nb--O bond of 2.18 Å because the dimension of a typical mono-oxo NbO_6 octahedron is 3.887 Å [33]. In order to preserve the valency of the Nb^{5+} cation (5.0 v.u.), the bond lengths of the four bridging Nb–O bonds must be about 2.06 Å and their bond strengths are 0.685 v.u. By analogy, a dioxo NbO_6 octahedron has two terminal Nb=O bonds, and the valency of these bonds adds to 3.50 v.u. and leaves 1.50 v.u. to be shared among the four remaining Nb–O bonds. This structure is not probable because there is no known NbO_6 reference compound with such a distorted niobate structure (see table 1). Thus, the dioxo NbO_6 and NbO_4 structures are not reasonable models for the highly distorted surface niobate species. The highly distorted surface niobate species is consistent only with the mono-oxo NbO_6 and/or NbO_4 models.

Of the mono-oxo NbO_6 and NbO_4 models for the highly distorted surface niobate species, the NbO_6 model is more reasonable in light of the structural chemistry of niobium oxide. Tetrahedrally coordinated niobate species are extremely rare, and NbO_4 tetrahedra appear only under extreme circumstances. For example, an NbO_4 tetrahedron may occur within a tetrahedral arrangement of oxygen atoms (referred to as a "hole") or cation defect site in a crystalline lattice, and is observed for the high-temperature modification of Nb_2O_5 [23]. Recent Raman studies of layered niobium oxide compounds also provide additional support to the mono-oxo NbO_6 model [33,34]. Structures with layers of regular NbO_6 octahedra terminate in highly distorted mono-oxo NbO_6 octahedra, similar to that of the NbO_6 surface model. When moisture is present between the niobate layers and the terminal Nb=O bond is solvated, the band occurs at 969 cm^{-1}. Upon dehydration, however, the band shifts to ~985 cm^{-1}, consistent with that observed for the highly distorted surface niobate species at 980 cm^{-1}. Therefore, consistent with the Raman studies of the layered niobate compounds, the mono-oxo NbO_6 model is more likely than the mono-oxo NbO_4 model as the highly distorted surface niobate species on alumina.

In summary, eqs. (3)–(5) have aided in elucidating a reasonable structure for the surface niobate species present in a 12 wt% Nb_2O_5/Al_2O_3 (63% of a monolayer) sample from its Raman spectrum. Comparison of the Raman spectra of the surface niobate species with those of aqueous niobate reference compounds showed that the hydrated system possesses surface $H_xNb_6O_{19}{}^{(8-x)-}$ polyoxoanions and these anions condense to form $Nb_{12}O_{36}$-like surface species upon dehydration. When dehydrated a highly distorted, mono-oxo NbO_6 octahedron is also present with its apical Nb=O bond at 1.706 ± 0.024 Å and remaining bonds estimated with an opposing Nb--O bond at 2.18 Å and four bridging Nb–O bonds at 2.06 Å. For both hydrated and dehydrated samples, a slightly distorted NbO_6 octahedron is present and its structure is independent of surface moisture; these attributes are consistent with a low-temperature form of bulk Nb_2O_5 or amorphous $Nb_2O_5 \cdot nH_2O$.

The empirical correlations between Raman stretching frequency and Nb–O bond length and bond strength are powerful tools for the interpretation of the Raman spectra of niobate species whose structures are distorted by a crystalline lattice or by a surface. In cases where diffraction techniques fall short of providing oxygen positions, Raman spectroscopy may be used to determine Nb–O bond distances for the niobate species. Knowledge of the bond distances of a niobate species can lead to information concerning its coordination and structure. Such an approach should popularize Raman spectroscopy as a complementary technique to diffraction methods in the structural studies of complex transition metal oxide systems.

6. Conclusions

An empirical correlation was established between Nb–O Raman stretching frequency and bond length. The correlation is based on measured Raman stretching frequencies and previously reported crystallographic Nb–O bond lengths. This correlation was further combined with Brown and Wu's empirical relation between Nb–O bond length and bond strength (in valence units) to arrive at a relation between stretching frequency and bond strength. These relations are presented graphically. These relationships are expected to provide insight into the structures of niobate species, especially for those chemical systems which are not amenable to analysis by diffraction or other spectroscopic techniques. In the present study, Raman stretching frequencies were predicted for the perfect NbO_4 and NbO_6 structures. The Nb–O bond distances of the NbO_6 octahedron in bismuth niobate, $BiNbO_4$, were determined as well as the structure of the surface niobate species in the Nb_2O_5/Al_2O_3 system. The Nb–O correlation is expected to aid in the structural determination of dehydrated surface niobate species on various oxide supports (γ-Al_2O_3, TiO_2, SiO_2, etc.), which are heterogeneous catalysts for many industrially important reactions.

Acknowledgement

Financial support from the Texaco Philanthropic Foundation and from the Sherman Fairchild Foundation is gratefully acknowledged by FDH. The authors further acknowledge the generous support of the Niobium Products Company (Pittsburgh, PA, USA).

References

[1] K. Nakamoto, Infrared and Raman spectra of inorganic and coordination compounds, 3rd Ed. (Wiley, New York, 1978).
[2] L. Dixit, D.L. Gerrard and H.J. Bowley, Appl. Spectrosc. Rev. 22 (1986) 189.
[3] I.E. Wachs, F.D. Hardcastle and S.S. Chan, Spectrosc. 1 (1986) 30.
[4] F.D. Hardcastle, I.E. Wachs, J.A. Horsley and G.H. Via, J. Mol. Catal. 46 (1988) 15.
[5] F.D. Hardcastle and I.E. Wachs, J. Mol. Catal. 46 (1988) 173.
[6] F.D. Hardcastle and I.E. Wachs, J. Phys. Chem., to be published.
[7] F.D. Hardcastle and I.E. Wachs, J. Raman Spectrosc. 21 (1990) 683.

[8] F.D. Hardcastle and I.E. Wachs, J. Solid State Chem., submitted for publication.

[9] J.I. Steinfeld, Molecules and radiation: An introduction to modern molecular spectroscopy (The MIT Press, Cambridge, 1981).

[10] P. Ayyub, M.S. Multani, V.R. Palkar and R. Vijayaraghavan, Phys. Rev. 34 (1986) 8137.

[11] C.N.R. Rao, Ind. J. Pure Appl. Phys. 16 (1978) 277.

[12] G.J. Blasse, Solid State Chem. 7 (1973) 169.

[13] E. Husson, Y. Repelin, N.Q. Dao and H. Brusset, J. Chem. Phys. 66 (1977) 5173.

[14] F.D. Hardcastle and I.E. Wachs, in preparation.

[15] I.D. Brown and K.K. Wu, Acta Cryst. B32 (1876) 1957.

[16] G.R. Somayajulu. J. Chem. Phys. 28 (1958) 814.

[17] G.R. Somayajulu, J. Chem. Phys. 28 (1958) 822.

[18] Y.P. Varshni, J. Chem. Phys. 28 (1958) 1081.

[19] D.R. Herschbach and V.W. Laurie, J. Chem. Phys. 35 (1961) 458.

[20] J.R. Bartlett and R.P. Cooney, J. Mol. Struct. 193 (1989) 295.

[21] I.D. Brown, Chem. Soc. Rev. 7 (1978) 359.

[22] H.D. Megaw, Acta Cryst. A24 (1968) 583.

[23] B.M. Gatehouse and A.D. Wadsley, Acta Cryst. 17 (1964) 1545.

[24] E.B. Wilson, Jr., J.C. Decius and P.C. Cross, Molecular vibrations: The theory of infrared and Raman spectra (Dover, New York, 1980).

[25] L. Pauling, General chemistry (Dover, New York, 1988).

[26] N. Galesic, B. Matkovic, M. Herceg and M. Sljukic, J. Less-Common Metals 25 (1971) 234.

[27] A.C. Skapski and D. Rogers, Chem. Commun. 23 (1965) 611.

[28] F.D. Hardcastle, Molecular structures of bulk and surface metal oxides by Raman spectroscopy: The diatomic approximation, Dissertation (Lehigh University, Bethlehem, PA, USA, 1990).

[29] J.-M. Jehng, Dissertation (Lehigh University, Bethlehem, PA, USA, 1990).

[30] T. Ikeya and M. Senna, J. Non-Cryst. Solids 105 (1988) 243.

[31] A. Goiffon and B. Spinner, Rev. Chim. Min. 11 (1974) 262.

[32] B. Spinner, Rev. Chim. Min. 5 (1968) 838.

[33] A.J. Jacobson, J.W. Johnson and J.T. Lewandowski, Inorg. Chem. 24 (1985) 3727.

[34] F.D. Hardcastle, I.E. Wachs, A.J. Jacobson and J.T. Lewandowski, unpublished results.

[35] J.M. Longo and P. Kierkegaard, Acta Chem. Scand. 20 (1966) 72.

[36] A.C. Sakowski-Cowley, K. Lukaszewicz and H.D. Megaw, Acta Cryst. B25 (1969) 851.

[37] L. Katz and H.D. Megaw, Acta Cryst. A22 (1967) 639.

[38] V.K. Trunov, V.A. Efremov, Y.A. Velikopodnyi and I.M. Averina, Sov. Phys. Crystallogr. 26 (1981) 35.

[39] V.A. Efremov, V.K. Trunov and A.A. Evdokimov, Soc. Phys. Crystallogr. 26 (1981) 172.